Rapid Communication J. Biochem. 121, 637-641 (1997)

Three-Dimensional Structure of *Escherichia coli* Branched-Chain Amino Acid Aminotransferase at 2.5 Å Resolution[1]

Kengo Okada,* Ken Hirotsu,*,[2] Mamoru Sato,† Hideyuki Hayashi,‡ and Hiroyuki Kagamiyama‡

*Department of Chemistry, Faculty of Science, Osaka City University, Sugimoto, Sumiyoshi-ku, Osaka 558; †Graduate School of Integrated Science, Yokohama City University, Kanazawa-ku, Yokohama 236; and ‡Department of Medical Chemistry, Osaka Medical College, Takatsuki, Osaka 569

Received for publication, January 16, 1997

The X-ray crystallographic structure of the branched-chain amino acid aminotransferase from *Escherichia coli* was determined by means of isomorphous replacement using the selenomethionyl enzyme as one of the heavy atom derivatives. The enzyme is a homo hexamer with D_3 symmetry, and the polypeptide chain of the subunit is folded into two domains (small and large domains). The coenzyme, pyridoxal 5′-phosphate, resides at the domain interface, its *re*-face facing toward the protein. The active site structure shows that the following sites can recognize branched-chain amino acids and glutamate as substrates: (1) a hydrophobic core formed by Phe36, Tyr164, Tyr31*, and Val109* for a branched-chain; (2) Arg97 for an acidic side chain of glutamate; and (3) Tyr95 and two main chain NH groups of Thr257 and Ala258 for the α-carboxylate of substrates. Although the main chain conformation of the active site is homologous to that of D-amino acid aminotransferase, many of the active site residues are different between them.

Key words: branched-chain amino acid aminotransferase, pyridoxal enzyme, substrate recognition, three-dimensional structure, X-ray crystallography.

Transamination plays an important role in amino acid metabolism. This reaction is catalyzed by aminotransferases, which require a pyridoxal 5′-phosphate (PLP) as a cofactor. Aspartate aminotransferases (AspAT) from several species have been extensively studied using biochemical, spectroscopic and X-ray crystallographic methods (*1-7*). Recently, the three-dimensional structure of pyridoxamine 5′-phosphate type D-amino acid aminotransferase (D-AAT), which exhibits no primary sequence homology with AspAT, has been solved (*8*). In spite of the different folding of D-AAT and AspAT, several amino acid residues essential for catalysis are commonly found in the two enzymes (Fig. 1).

The branched-chain amino acid aminotransferase [EC 2.6.1.42] (BCAT) from *Escherichia coli* reversibly catalyzes the transfer of α-amino groups of branched-chain amino acids to 2-oxoglutarate to form glutamate. The enzyme consists of six identical subunits, and each subunit is composed of 308 amino acid residues with a subunit molecular weight of 34,000, and has a covalently bound PLP (*9, 10*). BCAT exhibits a 28% amino acid sequence homology with D-AAT, implying that the folding topology of the polypeptide chains of the two enzymes are similar. However, BCAT and D-AAT are different in subunit assembly and substrate specificity (*10*). BCAT is in a hexameric form, catalyzes the transamination of L-amino acids, and is specific for branched-chain amino acids (L-isoleucine, L-leucine, and L-valine) and L-glutamate, while D-AAT is in a dimeric form, like AspAT, and catalyzes the transamination of a wide range of D-amino acids.

In AspAT and other aminotransferases, the catalytic Lys258 residue, which is the acceptor of α-proton of substrates, extends its side chain toward the *si*-face of PLP (*1*), while in D-AAT and BCAT, the proton transfer occurs on the *re*-face of PLP, as shown in Fig. 1 (*11*). Because of this *re*-face specificity, PLP in BCAT is expected to have the same orientation relative to the lysine residue as that in D-AAT. Therefore it is of great interest to compare the three-dimensional structures of D-AAT and BCAT in order to understand why, among L-amino acids, only branched ones share the same enzymatic transamination mechanism as D-amino acids. Here, we report an X-ray crystallographic study of BCAT in the PLP form.

The wild type BCAT was expressed in *Escherichia coli* (*9, 10*), and purified as previously described (*12*). Two different crystal forms were obtained in the presence of 100 mM HEPES (pH 7.5) and 200 mM $MgCl_2$ on vapor diffusion of hanging drops with 28% w/v polyethylene glycol (PEG) 400 as the precipitant. One belongs to the monoclinic space group, C2, with cell dimensions of $a=135.1$, $b=144.0$, $c=102.9$ Å and $\beta=136.1°$. The other, which is a

[1] This study was supported in part by a Grant-in-Aid for Scientific Research [No. 08214212 (Priority Areas)] from the Ministry of Education, Science, Sports and Culture of Japan, and a research grant from the Japan Society for the Promotion of Science ("Research for the Future Program").

[2] To whom correspondence should be addressed. Phone: +81-6-605-2557, Fax: +81-6-605-3131, E-mail: hirotsu@sci.osaka-cu.ac.jp

Abbreviations: AspAT, aspartate aminotransferase; BCAT, branched-chain amino acid aminotransferase; D-AAT, D-amino acid aminotransferase; EMTS, ethyl mercury thiosalicylate; PLP, pyridoxal 5′-phosphate; Tyr31*, the * indicates a residue from another subunit of the dimer unit.

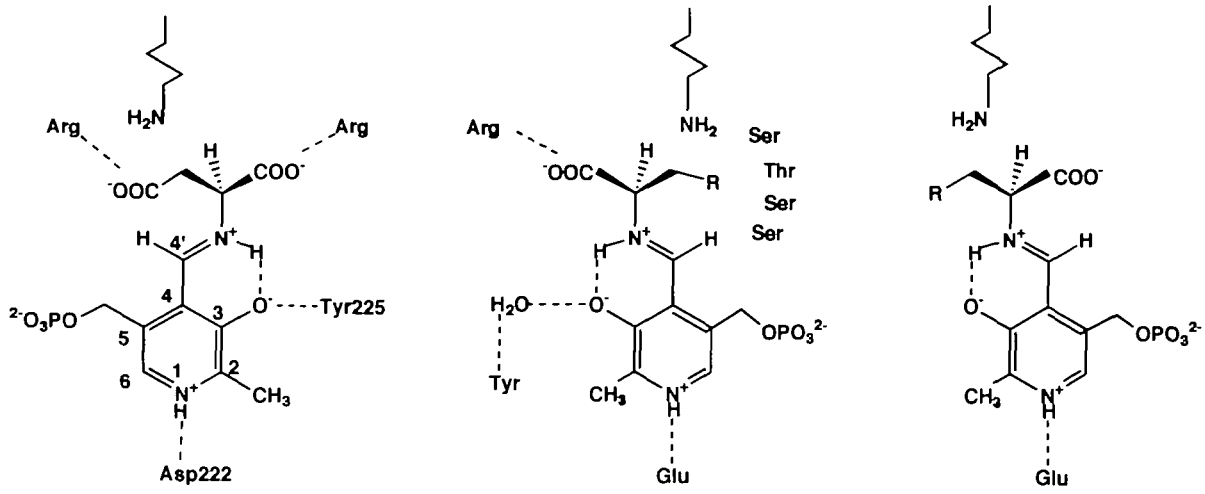

Fig. 1. **Schematic diagram of the orientation of the PLP-Schiff base and catalytic residue Lys viewed from the solvent region.** The α-proton of the substrate, which is abstracted by the Lys, is directed toward the inside of the active site pocket. The *si*-face of the coenzyme points toward Lys in AspAT and the *re*-face in D-AAT. BCAT has the same cofactor orientation as D-AAT (*8*), and the same substrate orientation as that of AspAT. In AspAT, the α- and β-carboxylates of the substrate, Asp, are recognized by two Arg residues. In D-AAT, the putative recognition sites for the α-carboxylate and side chain of the substrate are one Arg, one Thr, and three Ser residues.

TABLE I. **Data sets utilized for structure determination.**

Data set	Soak conditions[a]	Maximum resolution (Å)	Unique reflections	Completeness (%)	R_{merge} (%)	R_{diff}[b] (%)	No. of sites	Phasing power[c]
Native		2.5	39,622	83.5	5.9			
EMTS	1.0 mM, 18 h	2.8	31,039	91.7	8.2	12.5	3	0.9
SeMet[d]		2.4	50,192	91.8	5.1	11.0	21	0.7

[a]The soak time is given in hours (h). [b]$R_{diff} = \Sigma||F_{PH}| - |F_P||/\Sigma|F_P|$, where $|F_{PH}|$ and $|F_P|$ are the derivative and native structure-factor amplitudes, respectively. [c]Phasing power is the ratio of the root mean square (r.m.s) of the heavy atom scattering amplitude and the lack of closure error. [d]SeMet: selenomethionyl BCAT.

newly found form, belongs to the orthorhombic space group, $C222_1$, with cell dimensions of $a = 156$, $b = 101$, and $c = 142$ Å. Both crystals diffracted to 2.4 Å with a Rigaku RAXIS IIc, and to 1.8 Å with synchrotron radiation at the Photon Factory, KEK, Tsukuba (*13*). The self-rotation functions (*14*) computed with the native data for both crystals indicate one non-crystallographic 3-fold axis and two 2-fold axes consistent with the D_3 symmetry of BCAT having a crystallographic 2-fold axis and the presence of three subunits in an asymmetric unit.

Although many chemicals were used to prepare heavy atom derivatives for both crystal forms by means of soaking methods, no good derivative for the initial phasing was obtained except for the EMTS derivative of the monoclinic one. Selenomethionyl BCAT (seven selenium sites per subunit) was then prepared by overexpressing pUC119-*ilvE* in DL41(*metA*$^-$) cells grown in the presence of selenomethionine (*15*). The selenomethionyl protein was purified and crystallized like the wild type, two polymorphic crystals which are isomorphous with the monoclinic and orthorhombic forms of BCAT being obtained. The monoclinic crystal thus obtained was used for the phase determination.

Native data, BCAT-EMTS derivative data, and Se-Met-BCAT data were collected with an R-AXIS IIc with graphite-monochromated Cu-$K\alpha$ X-rays (40 kV, 100 mA), and processed and scaled using the programs, DENZO and SCALEPACK (*16*), respectively (Table I). The scaling of all data and map calculations were performed with the CCP4 program suite of programs (*14*). Three mercury sites were located using an isomorphous difference Patterson map calculated for the EMTS derivative. The positions of the 21 selenium sites were determined from difference Fourier maps based on mercury phasing. Refinement of the heavy atom parameters and calculation of the initial phases to 3.0 Å were performed with the program, MLPHARE (*14*). The phases were significantly improved by the process of solvent flattening (*17*), and local symmetry averaging (*18*) with the program, DM (*14*). The resulting map was of excellent quality and essentially the entire main chain conformation of one subunit could be traced (*19*). Those of the other two subunits in an asymmetric unit were obtained by taking advantage of the local 3-fold axis. Structure refinement was carried out by simulated annealing and energy minimization with non-crystallographic restraints using the program, XPLOR (*20*). The non-crystallographic symmetry constraints were lifted after the first round of refinement. The final R-factor and R-free, with 178 water molecules, were 18.8% for 37,577 reflections and 25.8% for 2,044 reflections, respectively, with

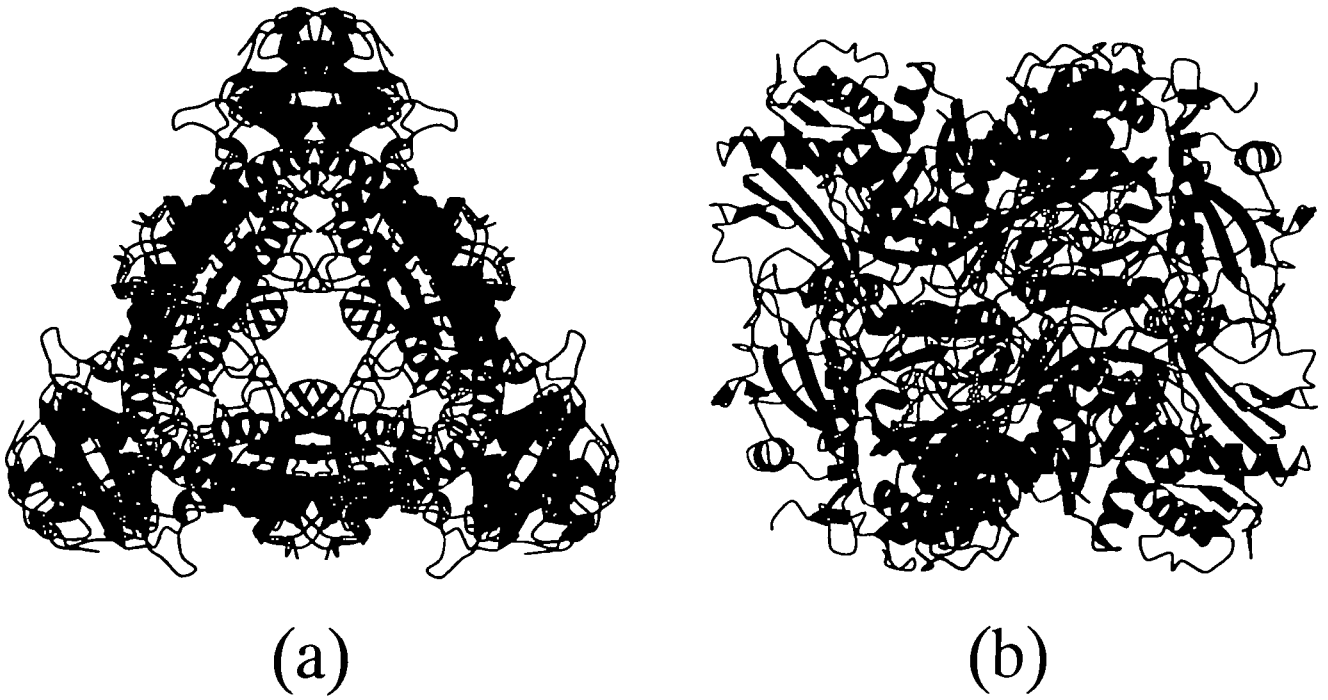

Fig. 2. **The overall hexameric structure of BCAT with the shape of a triangular prism, showing the six subunits in different colors.** The cofactors are shown in yellow as ball and stick models. (a) View of the molecule from the 3-fold axis. The upper half of the triangular prism consisting of three subunits (green, red, and purple) is related to the lower half by a 2-fold axis that is rectangular to a 3-fold axis. (b) View of the molecule along the 2-fold axis at the edge of the prism formed by the green and blue subunits. The 2-fold symmetric dimer unit (green and blue) is shown in the center, with another two dimer units (purple and orange, and red and gray) on the two sides.

$F > 2(\sigma(F))$ between 10.0 and 2.5 Å resolution. The final model lacks 3 N-terminal residues and the loop (Gly127 to Glu136) connecting the two domains. Analysis of the stereochemistry with PROCHECK (*21*) showed that 98.8% of the main chain atoms fall within the allowed region of the Ramachandran plot.

Figure 2 shows the overall hexameric structure of BCAT having the shape of a triangular prism. One side of the triangle is 87 Å and the height of the triangular prism is 79 Å. Each subunit in the hexamer interacts with the other four subunits. Among these interactions, the marked one is that between the two subunits related by the 2-fold axes at the edges of the triangular prism with a surface area of the subunit interface of about 5,400 Å^2. Thus, the hexamer can be regarded as the assembly of three dimer units around a 3-fold axis. The folding of this dimer unit is very similar to that of D-AAT as a dimeric molecule (*8*). Six active site cavities of BCAT are positioned on the three rectangular planes of the prism and face the solvent region.

Figure 3 shows a subunit structure with an ellipsoidal shape, including two loops from the other subunit of the dimer approaching the active site, PLP and the important residues in the active site. The subunit is divided into one small domain comprising the N-terminus to Trp126 and six C-terminal residues, and one large domain comprising Gln137 to Trp302. The small domain is characterized by an open twisted antiparallel β-sheet of six strands flanked by two α-helices on one side, and the large domain by a pseudo β-barrel structure consisting of two mixed β-sheets of five strands surrounded by three α-helices. The overall subunit structure is similar to that of D-AAT, except for the loop regions on the molecular surface.

The coenzyme, PLP, resides at the domain interface and at the bottom of the active site pocket. The active site comprises residues from both domains of one subunit and the small domain (two loops shown in red in Fig. 3) of the other subunit of the dimer unit. Figure 4 is a schematic drawing of the active site structure of BCAT. The orientation of PLP in BCAT is identical to that in D-AAT but different from that in AspAT (*1, 8*). Lys159 lies on the *re*-face of the coenzyme in BCAT, confirming the earlier proposal that Lys159 is the base located on the *re*-face of PLP and abstracts α-protons (*11*). PLP of BCAT forms a Schiff base with Lys159, and is sandwiched between Gly196-Glu197 and Leu217 from above and below. Glu193 forms an ion pair with the protonated nitrogen atom of the pyridine ring of PLP, and is considered to strengthen the electron withdrawing effect of the pyridine ring of PLP as an electron sink, as has been observed for Asp222 of AspAT (*22, 23*). Tyr164 is hydrogen bonded to O3′ of PLP, which is reminiscent of the fine-tuning effect of Tyr225 of AspAT on the electronic state of PLP (*24, 25*). The two residues, Lys159 and Glu193, are also conserved in D-AAT. The direct hydrogen bond between Tyr and O3′ is not conserved in D-AAT, but the hydrogen bond network, Tyr---H_2O---O3′, may be used in place of the direct one (*8*).

Upon binding of a substrate, PLP forms a new Schiff base with the substrate, and an α-proton of the substrate is directed toward the catalytic residue, Lys, indicating that the side chain and α-carboxylate of the substrate bound to the active site of BCAT are on the sides of O3′ and the phosphate group of PLP, respectively (Fig. 1). The most

Fig. 3. **The overall subunit structure of BCAT showing β-strands (green), α-helices (orange), and loops (white).** The small and large domains comprise the upper and lower parts of this figure, respectively. PLP (yellow) is located at the bottom of the active site pocket with its *re*-face toward the protein. The active site cleft is constructed from residues from both domains of one subunit, and residues (Tyr31* and Val109*) from two loops (red) of the other subunit of the dimer unit. Only selected residues of the active sites are shown for clarity.

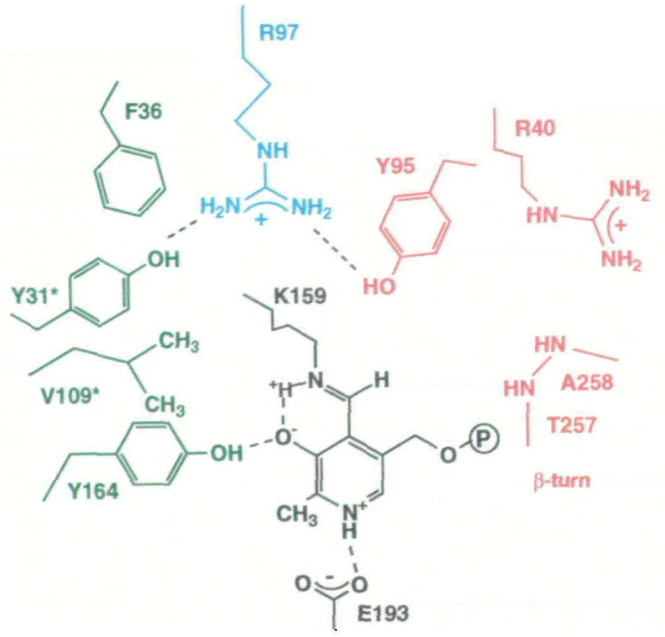

Fig. 4. **Schematic drawing of the active site of BCAT.** Only the critical residues for the catalytic action and substrate recognition are shown. The most plausible recognition sites for hydrophobic side chains, acidic side chains, and α-carboxylate of the substrate amino acids are shown in green, blue, and red, respectively.

plausible recognition site for the hydrophobic side chain of Leu, Ile, or Val as a substrate is the hydrophobic core formed by Phe36, Tyr164, Tyr31* (* means this residue is from the other subunit of the dimer) and Val109* (Fig. 4). The corresponding candidate for the acidic side chain of Glu as a substrate is Arg97, which forms a hydrophilic site with Tyr31* and Tyr95. The hydrophobic recognition site is adjacent to the hydrophilic recognition site due to its sharing Tyr31*. The substrate will interact with one of these two sites by adjusting its side chain conformation without a large conformational change in the active site residues, although, at the present stage, the details of the recognition mechanism that distinguishes between the hydrophobic and acidic side chains are unknown. At first glance, the α-carboxylate of the substrate appears to be recognized by Arg40, just like in the case of AspAT. However, Arg40, which interacts with Glu260 and faces the solvent region, is blocked from the active site pocket by the wall formed by Tyr95 and the β-turn comprising Gly256-Thr257-Ala258-Ala259. An alternative candidate for the α-carboxylate recognition site is three hydrophilic groups comprising OH of Tyr95 and two main chain NH groups of Thr257 and Ala258, which point toward the inner side of the active site pocket. Preliminary X-ray analysis of the BCAT in complex with 4-methylvaleric acid showed that these three groups actually interact with the carboxylate of the inhibitor (unpublished result).

When the active site of BCAT is compared with that of D-AAT, almost all the residues of D-AAT necessary for substrate recognition and other residues forming the active site pocket can be seen not to be conserved except for the catalytically-critical residues, Lys159 and Glu193 (*8*). The corresponding active site residues in the primary structures of BCAT and D-AAT are as follows: Tyr31* (Phe in D-AAT), V109* (His), Phe36 (Tyr), Tyr164 (Leu), Arg97 (Tyr), Tyr95 (His), Gly256 (Ser), Thr257 (Thr), Ala258 (Thr), Ala259 (Ser), Arg40 (Lys), Gly196 (Ser), Glu197 (Ser), and Leu217 (Leu). Nevertheless, the main chain conformation is conserved: the main chain atoms (66 atoms) of the active site residues of BCAT fit those in D-AAT with an r.m.s. deviation of 0.54 Å. This indicates that the change in substrate specificity from an L-amino acid to the enantiomer, a D-amino acid, can be attained only through the replacement of active site residues, without a change in the main chain conformation. From the viewpoint of designing new functional proteins by means of protein engineering, therefore, an enantiomeric change in substrate specificity is expected to be difficult compared with a change in the side chain specificity, because many residues must be properly replaced.

The refinement of the structure of the orthorhombic form at higher resolution using synchrotron radiation, and structure determination of BCAT in complexes with 4-methylvaleric acid and 2-methylleucine are in progress. These studies will provide essential information for a general understanding of the substrate recognition and the reaction mechanism of aminotransferases.

We wish to thank Prof. W.A. Hendrickson of Columbia University, and Prof. Y. Mitsui and Dr. T. Senda of Nagaoka University of Technology for providing the new auxotrophic strain, DL41.

REFERENCES

1. Christen, P. and Metzler, D.E., eds. (1985) *Transaminases*, Wiley and Sons, New York
2. Mcphalen, C.A., Vincent, M.G., and Jansonius, J.N. (1992) X-ray structure refinement and comparison of three forms of mitochondrial aspartate aminotransferase. *J. Mol. Biol.* **225**, 495-517
3. Malashkevich, V.N., Toney, M.D., and Jansonius, J.N. (1993) Crystal structures of true enzymatic reaction intermcdiates: aspartate and glutamate ketimines in aspartate aminotransferase. *Biochemistry* **32**, 13451-13462
4. Malashkevich, V.N., Strokopytov, B.V., Borisov, V.V., Dauter, Z., Wilson, K.S., and Torchinsky, Y.M. (1995) Crystal structure of the closed form of chicken cytosolic aspartate aminotransferase at 1.9 Å resolution. *J. Mol. Biol.* **247**, 111-124
5. Jäger, J., Moser, M., Sauder, U., and Jansonius, J.N. (1994) Crystal structures of *Escherichia coli* aspartate aminotransferase in two conformations. Comparison of an unliganded open and two liganded closed forms. *J. Mol. Biol.* **239**, 285-305
6. Okamoto, A., Higuchi, T., Hirotsu, K., Kuramitsu, S., and Kagamiyama, H. (1994) X-Ray crystallographic study of pyridoxal 5′-phosphate-type aspartate aminotransferase from *Escherichia coli* in open and closed form. *J. Biochem.* **116**, 95-107
7. Miyahara, I., Hirotsu, K., Hayashi, H., and Kagamiyama, H. (1994) X-Ray crystallographic study of pyridoxamine 5′-phosphate-type aspartate aminotransferase from *Escherichia coli* in three forms. *J. Biochem.* **116**, 1001-1012
8. Sugio, S., Petsko, G.A., Manning, J.M., Soda, K., and Ringe, D. (1995) Crystal structure of a D-amino acid aminotransferase: How the protein controls stereoselectivity. *Biochemistry* **34**, 9661-9669
9. Kuramitsu, S., Ogawa, T., Ogawa, H., and Kagamiyama, H. (1985) Branched-chain amino acid aminotransferase of *Escherichia coli*: nucleotide sequence of the *ilvE* gene and the deduced amino acid sequence. *J. Biochem.* **97**, 993-999
10. Inoue, K., Kuramitsu, S., Aki, K., Watanabe, Y., Takagi, T., Nishigai, M., Ikai, A., and Kagamiyama, H. (1988) Branched-chain amino acid aminotransferase of *Escherichia coli*: overproduction and properties. *J. Biochem.* **104**, 777-784
11. Yoshimura, T., Nishimura, K., Ito, J., Esaki, N., Kagamiyama, H., Manning, J.M., and Soda, K. (1993) Unique stereospecificity of D-amino acid aminotransferase and branched-chain L-amino acid aminotransferase for C-4′ hydrogen transfer of the coenzyme. *J. Am. Chem. Soc.* **115**, 3897-3900
12. Kamitori, S., Odagaki, Y., Inoue, K., Kuramitsu, S., Kagamiyama, H., Matsuura, Y., and Higuchi, T. (1989) Crystallization and preliminary X-ray characterization of branched-chain amino acid aminotransferase from *Escherichia coli*. *J. Biochem.* **105**, 671-672
13. Sakabe, N., Ikemizu, S., Sakabe, K., Higashi, T., Nakagawa, A., Watanabe, N., Adachi, S., and Sasaki, K. (1995) Weissenberg camera for macromolecules with imaging plate data collection system at the Photon Factory: Present status and future plan (invited). *Rev. Sci. Instrum.* **66**, 1276-1281
14. Collaborative Computational Project, Number 4. (1994) The CCP4 suite: program for protein crystallography. *Acta Crystallogr.* **D50**, 760-763
15. Hendrickson, W.A., Horton, J.R., and LeMaster, D.M. (1990) Selenomethionyl proteins produced for analysis by multiwavelength anomalous diffraction (MAD): a vehicle for direct determination of three-dimensional structure. *EMBO J.* **9**, 1665-1672
16. Otwinowski, Z. (1993) Data collection and processing in *Proceedings of the CCP4 Study Weekend*, pp. 56-62, SERC Daresbury Laboratory, Warrington
17. Wang, B.-C. (1985) Resolution of phase ambiguity in macromolecular crystallography. *Methods Enzymol.* **115**, 90-112
18. Bricogne, G. (1974) Geometric sources of redundancy in intensity data and their use for phase determination. *Acta Crystallogr.* **A42**, 140-149
19. Jones, T.A., Zou, J.-Y., Cowan, S.W., and Kjeldgaard, M. (1991) Improved methods for building protein models in electron density maps and the location of errors in these models. *Acta Crystallogr.* **A47**, 110-119
20. Brünger, A.T., Kuriyan, J., and Karplus, M. (1987) Crystallographic R factor refinement by molecular dynamics. *Science* **235**, 458-460
21. Laskowski, R.A., MacArthur, M.W., Moss, D.S., and Thornton, J.M. (1993) PROCHECK: A program to check the stereochemical quality of protein structures. *J. Appl. Crystallogr.* **26**, 283-291
22. Yano, T., Kuramitsu, S., Tanase, S., Morino, Y., and Kagamiyama, H. (1992) Role of Asp222 in the catalytic mechanism of *Escherichia coli* aspartate aminotransferase: The amino acid residue which enhances the function of the enzyme-bound coenzyme pyridoxal 5′-phosphate. *Biochemistry* **31**, 5878-5887
23. Yano, T., Hinoue, Y., Chen, V.J., Metzler, D.E., Miyahara, I., Hirotsu, K., and Kagamiyama, H. (1993) Role of an active site residue analyzed by combination of mutagenesis and coenzyme analogue. *J. Mol. Biol.* **234**, 1218-1229
24. Inoue, K., Kuramitsu, S., Okamoto, A., Hirotsu, K., Higuchi, T., Morino, Y., and Kagamiyama, H. (1991) Tyr225 in aspartate aminotransferase: contribution of the hydrogen bond between Tyr225 and coenzyme to the catalytic reaction. *J. Biochem.* **109**, 570-576
25. Goldberg, J.M., Swanson, R.V., Goodman, H.S., and Kirsch, J.F. (1991) The tyrosine-225 to phenylalanine mutation of *Escherichia coli* aspartate aminotransferase results in an alkaline transition in the spectrophotometric and kinetic pK_a values and reduced values of both k_{cat} and K_m. *Biochemistry* **30**, 305-312